

# A Crosstalk Study on CMOS Active Pixel Sensor Arrays for Color Imager Applications

Ching-Chun Wang, and Charles G. Sodini

Department of Electrical Engineering and Computer Science, Massachusetts Institute of Technology  
77 Massachusetts Avenue, Bldg.38-265, Cambridge, MA 02139, U.S.A.  
Phone: 1-617-2530711, Fax: 1-617-2530520, E-mail: chcwang@mit.edu

## Abstract

The crosstalk phenomena of CMOS image sensors is studied with a 64 x 64 N-well active pixel sensor (APS) array. The pixel size is  $4 \times 4 \mu\text{m}^2$  and the array is fabricated using a  $0.25 \mu\text{m}$  STI CMOS process with  $8 \mu\text{m}$  thick epi wafers. The major crosstalk mechanism is identified to be minority carrier diffusion. The crosstalk amplifies the color mismatch due to intrinsic pixel noise and degrades the color performance under low illumination. Process and layout improvements for minimizing crosstalk are proposed.

## Introduction

CMOS imagers have attracted the attention of the solid-state imaging market due to their superior circuit integration ability and lower power consumption compared with CCD imagers[1]. Since typical CMOS processes are originally optimized for digital circuit operation, process modifications have been proposed to improve sensor parameters, such as leakage current, for imaging applications[2][3].

The latest developments on imagers show decreasing pixel size in order to simultaneously achieve higher spatial resolution and maintain a reasonable chip size. As pixel size continues to shrink, significant crosstalk between pixels emerges[4]. This crosstalk phenomena reduces the effective spatial resolution and amplifies the pixel-to-pixel color mismatch for an imager with a mosaic color filter pattern. In this study, the crosstalk mechanism is studied by using an N-well APS array with a hollow metal shield, which exposes a single pixel in the center of the array and covers the others. Matching between experimental results and device simulations indicates that minority carrier diffusion is the main crosstalk mechanism. The measured data is used to study the amplification effect of the pixel-to-pixel color mismatch induced by crosstalk. Process and layout improvements are proposed to reduce the crosstalk.

## Fabrication of the sensor array

A 64 x 64 3-T N-well active pixel sensor (APS) array is fabricated using a non-silicide source/drain  $0.25 \mu\text{m}$  STI CMOS process. The characteristics of the array are shown in Table 1. An N-well photodiode structure is uti-

lized in this experiment for its superior performance over the  $\text{N}^+/\text{PW}$  photodiode in this process[3]. All pixels, with the exception of the center pixel, are optically shielded with the metal-3 layer. Row decoders, column decoders and analog buffers are implemented on chip for signal readout.

## Results and Discussion

The crosstalk measurement is performed with optical wavelengths varying from 400nm to 900nm. Varying optical intensity within pixel saturation region shows little impact on the crosstalk data. Fig. 1 shows the measured crosstalk for the nearest neighbors of the exposed pixel. The crosstalk value is defined as the ratio between the signal of the shielded pixels and that of the exposed pixel. The value is higher at longer wavelengths. Since the long-wavelength photons penetrate deeper into Si, the wavelength dependence of crosstalk suggests that minority carrier diffusion could be an important mechanism. The mechanism is schematically shown in Fig. 2. Most of the photo-carriers generated in the depletion region are driven by the electric field and collected by the exposed photodiode. The carriers generated deep in the  $\text{P}^+$  substrate are recombined efficiently due to the short minority carrier lifetime. The carriers generated between the depletion region and the  $\text{P}^+$  substrate diffuse either back to the exposed photodiode or to the adjacent pixels. A 2-D device simulation is performed with the N-well doping profile of this process and the result is shown in Fig. 3. The trend of the simulation result matches well with the measured data. As expected, the simulated crosstalk is generally higher than the measured crosstalk since the impact of optical blockage and carrier absorption by the pixel transistors is not considered in the simulation. The higher measured crosstalk at short wavelength is attributed to obliquely injected light from optical diffraction or metal layer reflection. The exposed window being larger than the size of the photodiode also contributes to crosstalk. According to simulation, as the size of the exposed window is reduced to the size of the photodiode, the crosstalk value at around 400 – 450nm drops to nearly zero.

The quantum efficiency (QE) of the exposed pixel is measured and shown in Fig. 4. As the crosstalk compo-

nents from the eight nearest neighbors are taken into account, the summed QE matches well with the one measured from the arrays with no metal-3 shield. The peaks of the QE curves shift by roughly 20nm due to the difference of the dielectric thickness on the two chips. This result validates photo-carrier conservation and shows that a significant portion of the QE measured with typical methods comes from crosstalk.

The crosstalk data is utilized to study the color error amplification effect. In order to estimate the amplification factor, two assumptions are made. First, it is assumed that the color filters are arranged in a R/G/B Bayer pattern. Second, the spectral responses of the R/G/B pixels are proportional to the color-matching functions of the CIE 1931 standard colorimetric observers[5]. The first assumption is based on a well-known example of color filter configuration; the second is made to simplify color coordinate mapping from the pixel outputs onto a standard color space. Based on the measured crosstalk data and the aforementioned assumptions, the spectral responses for the R/G/B pixels with crosstalk are calculated and shown in Fig. 5. The ideal spectral response curves without crosstalk are also shown for comparison. In the calculation, crosstalk from the eight nearest neighbors are considered. The calculation procedure is described with the following example. The color filter pattern is shown at the upper right corner of Fig. 5. A blue pixel is surrounded by four green pixels as adjacent neighbors and four red pixels as diagonal neighbors. Due to crosstalk, the blue pixel exchanges photo-carriers with its neighbors. The amount of carrier exchange is further modulated by the spectral responses of the corresponding color filters. As a result, the peak value of the spectral response for the blue pixel drops and, conversely, the response increases at the higher transmission wavelengths of the green and red pixels. Similar computations are executed for green and red pixels to achieve the R/G/B spectral response curves. The curves are distorted from the ideal response curves due to crosstalk.

These responses are denoted as  $\bar{x}(\lambda)$ ,  $\bar{y}(\lambda)$ , and  $\bar{z}(\lambda)$  respectively for red, green and blue pixels. Using the models developed in color science, these functions can be utilized to calculate the tristimulus values of color stimulus. For a specific color stimulus with spectral distribution  $p(\lambda)$ , the tristimulus values can be calculated from

$$X = k \int p(\lambda) \bar{x}(\lambda) d\lambda,$$

$$Y = k \int p(\lambda) \bar{y}(\lambda) d\lambda,$$

$$Z = k \int p(\lambda) \bar{z}(\lambda) d\lambda,$$

where the integration range is the visible wavelengths ( $\sim 380\text{nm} - 780\text{nm}$ ) and  $k$  is a normalizing factor. The tristimulus values can be transformed onto a standard color space named the 1976 CIE Uniform Chromaticity Scales (UCS) diagram as shown in Fig. 6. The distribution of color on this diagram is nearly uniform; therefore, the distance between two color coordinates represents a measurement of the color difference. The coordinate  $(u', v')$  on the diagram represents a specific color and can be calculated by

$$u' = \frac{4X}{X + 15Y + 3Z}, \text{ and } v' = \frac{9Y}{X + 15Y + 3Z}.$$

For monochromatic light,  $p(\lambda)$  becomes a delta function  $\delta(\lambda - \lambda_0)$  and the tristimulus values  $X$ ,  $Y$ , and  $Z$  are proportional to the spectral responses of  $\bar{x}(\lambda_0)$ ,  $\bar{y}(\lambda_0)$ , and  $\bar{z}(\lambda_0)$  at a specific wavelength  $\lambda_0$ . Utilizing the above formula, the color coordinates  $(u', v')$  for the monochromatic light on the UCS diagram are calculated and located on the curves shown in Fig. 6. Since a general color stimulus is a linear combination of monochromatic light with positive  $p(\lambda)$ , its corresponding color coordinate, after applying the math, will be encircled by the curve of the monochromatic light. Thus, the closed area formed by the monochromatic light constitutes a complete color space for human visual perception.

The two closed areas shown on Fig. 6 represent the color gamuts of the ideal color pixels and the pixels with the crosstalk effect. Due to crosstalk, the color gamut shrinks. In order for the displaying systems to correctly present color, a standardized color space is necessary. That means an ideal color correcting process exists to map the distorted color coordinates back to the original. This operation is essentially an amplification process. Since the area ratio of the two color gamuts is approximately 3:1, this mapping process will amplify pixel-to-pixel color error due to intrinsic pixel noise, on average, by a factor of  $\sqrt{3}$ .

The noise sources of color mismatch are also analyzed to understand when the amplification effect has significant impact. Theoretically, the noise components include both temporal and spatial noise. However, the mismatch produced by fixed pattern noise (FPN) usually dominates and is more significant than that produced by random noise because color mismatch by FPN cannot be averaged out with fast refreshed image frames by human eyes. Column-to-column FPN is typically caused by circuit mismatch and is easier to fix. Pixel-to-pixel FPN (P-

P FPN) is typically determined by process characteristics and is difficult to correct without a frame buffer. In order to characterize P-P FPN, an unshielded pixel array is utilized so that the amount of crosstalk is uniform across the array and has no impact on the P-P FPN measurement. The measured P-P FPN and its ratio with the average signal at various illumination levels are shown in Fig. 7. The non-zero P-P FPN at low illumination is mainly due to dark current mismatch of the pixels; the linear response of P-P FPN versus illumination is due to mismatch of photo-sensing area and capacitance. The ratio between P-P FPN and the average signal defines a normalized noise level. This level increases significantly as the illumination on the imager surface falls below 5 lux, causing a worse color mismatch amplified by crosstalk.

There are several approaches to minimize the crosstalk. First, a shallow epi wafer forces the carriers generated deep in the substrate to recombine efficiently and thus reduces the probability for the carriers to diffuse to the other pixels. This approach is more effective for long-wavelength photons. Second, a smaller opening of the metal shield assures all photons fall on the photodiodes. This method minimizes the number of photo-generated carriers near the pixel boundary and is effective for reducing crosstalk at all wavelengths. Simulations show that crosstalk values lower than 2% in the entire visible light spectrum can be achieved for a 2 $\mu$ m epi wafer with all photons falling within the photodiode region. However, both approaches degrade the sensitivity since either the available photo-generated carriers or the incoming photon flux is reduced.

### Summary

The crosstalk mechanism of CMOS image sensors is studied on a 64 x 64 N-well APS array with a hollow metal shield pattern. Minority carrier diffusion is the major contributing mechanism for crosstalk. Due to crosstalk, the pixel-to-pixel color mismatch is degraded. Finally, process and layout improvements for minimizing crosstalk are proposed.

### Acknowledgments

The authors would like to thank the CIS team at R&D dept., Taiwan Semiconductor Manufacturing Company, Ltd. and the Center for Integrated Circuits and Systems at MIT for their support.

### References

- [1] E. R. Fossum, Trans. ED, ED-44, 1997, pp.1689-1698
- [2] H.-S. P. Wong, IEDM Tech. Dig., 1997, pp.201-204
- [3] S.-G. Wu, et al., IEDM Tech. Dig., 2000, pp.705-708
- [4] M. Furumiya, et al., IEDM Tech Dig., 2000, pp.701-704

- [5] G. Wyszecki and W. S. Stiles, "Color science – concepts and methods, quantitative data and formulas", 2nd ed., Wiley, 1982

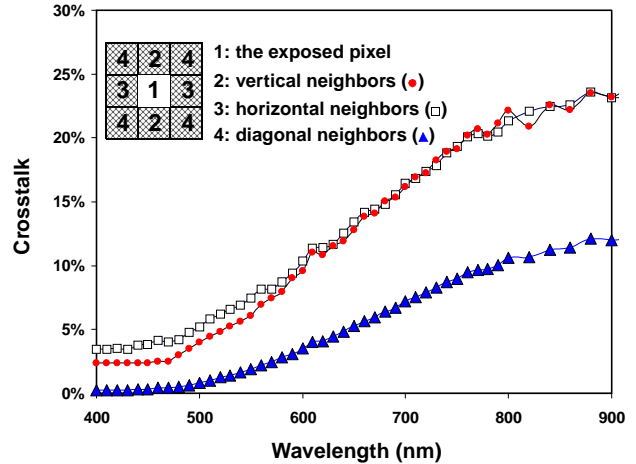


Figure 1: Measured crosstalk versus wavelength for the adjacent pixels along the horizontal (empty square), vertical (solid circle), and diagonal directions (triangle).

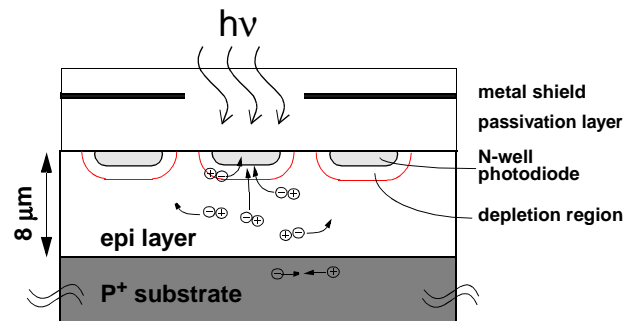


Figure 2: Minority carrier diffusion mechanism.

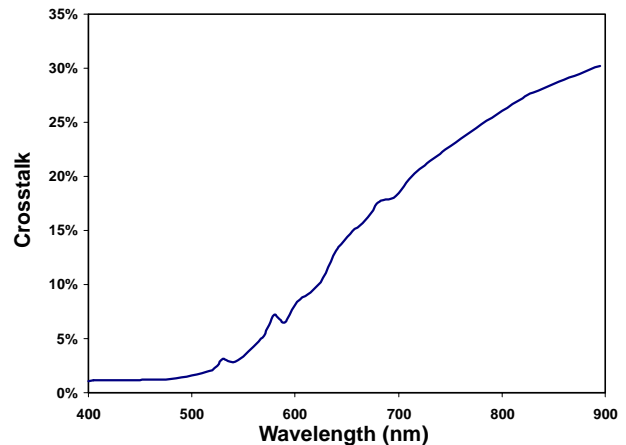


Figure 3: Crosstalk versus wavelength from the 2-D device simulation. The bumps on the curve is due to the empirical Si absorption coefficient, which does not monotonically decrease with wavelength.

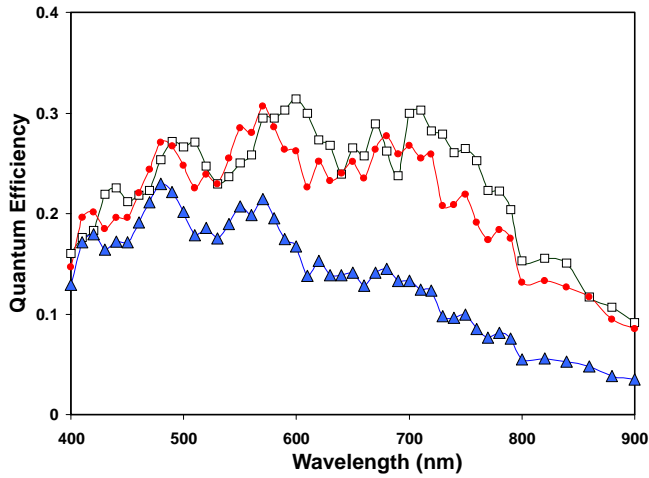


Figure 4: Quantum efficiencies (QE) of the pixels. Triangle: QE of the exposed pixel; solid circle: QE of the exposed pixel plus crosstalk from nearest neighbors; empty square: QE of the pixels for the array with no metal shield pattern.

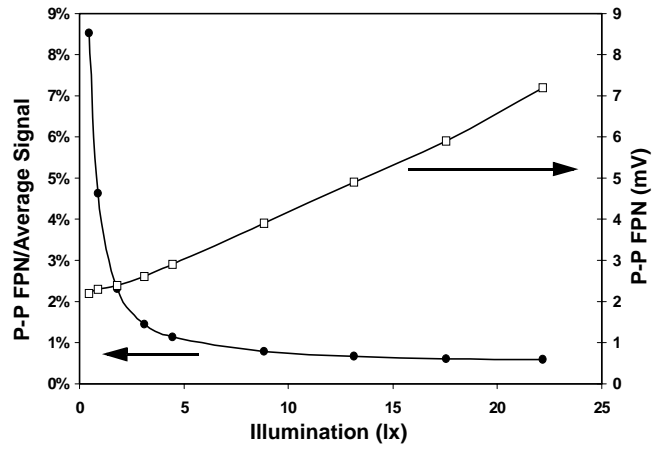


Figure 7: Pixel-to-pixel fixed pattern noise (empty square) versus illumination and the normalized P-P FPN with the average signal (solid circles) versus illumination. Integration time: 30ms.

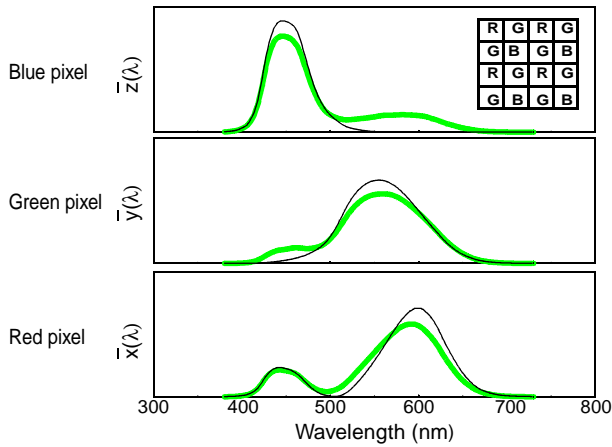


Figure 5: Spectral response curves of the R/G/B pixels with (thick line) and without crosstalk (thin line). The upper right corner shows the schematic of Bayer color-filter pattern.

Process	0.25 $\mu\text{m}$ non-silicide source/drain STI CMOS process
Format	64 x 64
Pixel size	4 x 4 $\mu\text{m}^2$
Sensor type	NW/Psub photodiode
Fill factor	~ 25%
Sensitivity	1.7 V/lx/sec
Leakage current	0.35 fA/pixel/sec @ 25°C
Conversion gain	33 $\mu\text{V}/\text{electron}$

Table 1: The characteristics of the APS array in the experiments.

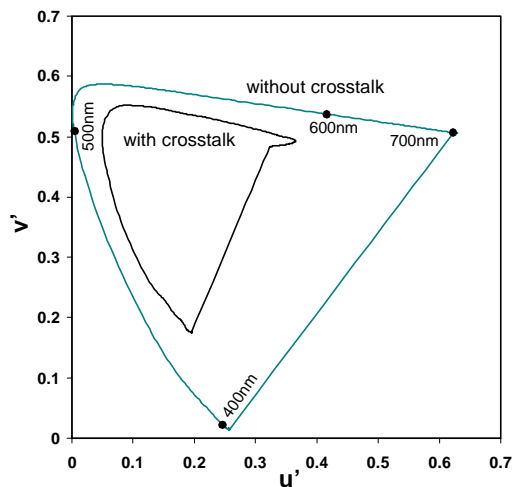


Figure 6: Color gamuts with and without crosstalk on the 1976 CIE Uniform Chromaticity Scales diagram.